

# Formation of long nanosecond rectangular pulses in the active RF pulse compression system with a compact resonant cavity

S N Artemenko<sup>1</sup>, S A Gorev, V S Igumnov<sup>2</sup> and Yu G Yushkov

National Research Tomsk Polytechnic University, Tomsk, Russia

Email: <sup>1</sup>snartemenko@mail.ru, <sup>2</sup>vladislavigumnov@yahoo.com

**Abstract.** This work presents the results of the study of an active microwave pulse compression system capable of forming the rectangular pulses with duration ~10-100 ns, while its dimensions are several times smaller than the radiated wave train. Such compression system is based on the compact planar-voluminal resonant cavity constructed in the shape of a meander from waveguide sections and H-plane tees. The resonant cavity sections are parallel and are in the same plane with tees. The energy input element is located in the input end of the first section. The output device designed as an H-plane tee interference switch is connected to the output end of the last section. Each end of remaining sections is connected through a straight arm to an H-tee with a short-circuited quarter-wave second straight arm. The side arm of each tee is connected with the side arm of the tee in the next section, thus coupling the sections. The short-circuited arm provides the "open" mode and transmission of the wave from tee to tee. We determined the expressions for wave amplitudes in the components of the meander resonant cavity made of three sections and analyzed the expressions as the functions of the parameters determining the oscillation range and energy distribution in the resonant cavity. Experiments demonstrated that under certain conditions the compressors with such resonant cavity could generate nearly rectangular pulses with duration equal to the time of wave two-way traveling along the resonant cavity, and with the power compatible with that of the wave in the resonant cavity, and the length of the radiated wave train several-fold exceeding the size of the compressor. At pulse duration equal to 25 ns, the gain coefficient was 13 dB and pulse power was 40 MW. The work demonstrates the possibility to change the geometry of the resonant cavity by rearranging its components without changing the output pulse parameters.

## 1. Introduction

Work [1] describes the concept of active microwave pulse compressions systems which, being of a relatively small size, are capable of forming rectangular nanosecond RF pulses with the radiated wave train length several times exceeding the compression system dimensions. The concept is based on replacing a traditional energy-storing resonant cavity with a structured resonant system with variable geometry. The structural element of the system is replaced with a one- or moderately multimode waveguide section with H-plane tees or their analogues on both ends and a resonant length. Such elements with limiting tees with a shorted straight arm and a free side arm can transmit a working wave with very little reflection. This feature of structure elements and the capability of the tees to change the wave direction allow us to build compact storage systems with a relatively long time of



working wave travel. When energy is extracted via an interference RF switch on the system's output port, this time determines the duration of the output rectangular pulse.

Paper [1] presents the first results of the experimental study of a microwave pulse compression system operating on the basis of the proposed concept and equipped with a resonant system made of two waveguide sections assembled as a meander half-period. The work demonstrates the compression system performance: practically rectangular pulses with duration 15 ns, gain 15 dB and power 60 MW were formed at 2800 MHz. The length of the radiated wave train four times exceeded the compression system dimensions.

This work contributes to the development of the concept by studying the RF compression system similar to one studied in the work [1] and by designing the form of a meander using three rather than two waveguide sections connected through limiting H-tees, as shown in Figure 1. The study focuses on the specific details of the work of such compression systems.

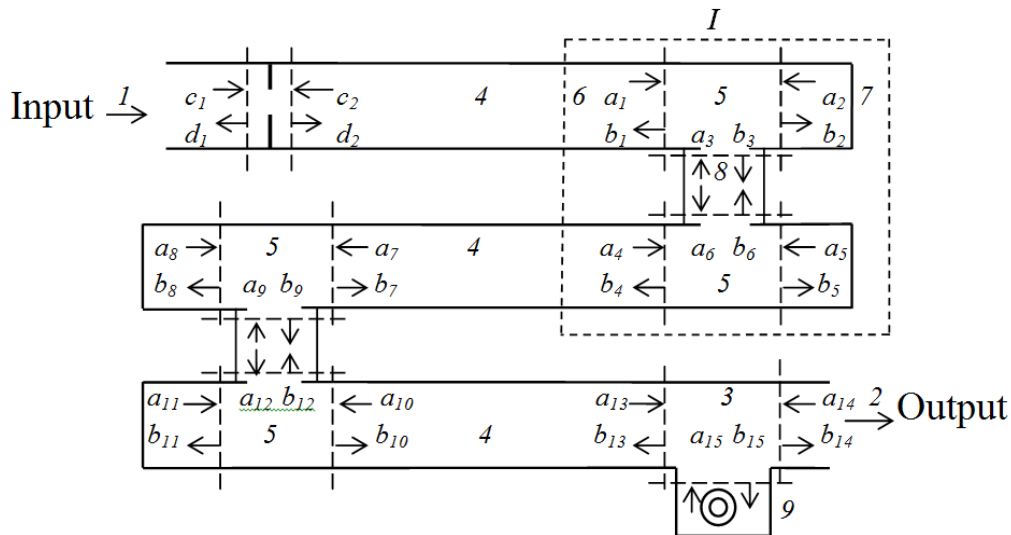


**Figure 1.** Schematic of the active microwave compression system with a compact storage cavity in the form of a meander. 1 – the input port with the energy input element; 2 – the output port with the energy extraction device 3; 4 – the waveguide sections; 5 – limiting H-tees with an input straight arm 6, a short-circuited second straight arm 7 and a shared side arm 8; 9 – the microwave switch.

## 2. Analysis

Particular interest represent those characteristics of the system, which determine the parameters of compression system input pulses. Thus, we need to determine the dependencies of wave amplitudes in system elements from the electrical length of the component parts of each element. These amplitudes show the energy distribution in the system and substantially influence the pulse power and the shape. Also, we need to determine the range of oscillations in the system and the energy distribution by oscillations depending on the section and tee arms lengths.

The analysis will be performed using the dispersion matrix method [2], where we can write down the following equations for the necessary amplitudes:

$$\begin{pmatrix} d_1 \\ d_2 \end{pmatrix} = S_1 \begin{pmatrix} c_1 \\ c_2 \end{pmatrix}, \begin{pmatrix} b_1 \\ b_2 \\ b_3 \end{pmatrix} = S_2 \begin{pmatrix} a_1 \\ a_2 \\ a_3 \end{pmatrix}, \begin{pmatrix} b_4 \\ b_5 \\ b_6 \end{pmatrix} = S_2 \begin{pmatrix} a_4 \\ a_5 \\ a_6 \end{pmatrix}, \begin{pmatrix} b_7 \\ b_8 \\ b_9 \end{pmatrix} = S_2 \begin{pmatrix} a_7 \\ a_8 \\ a_9 \end{pmatrix}, \begin{pmatrix} b_{10} \\ b_{11} \\ b_{12} \end{pmatrix} = S_2 \begin{pmatrix} a_{10} \\ a_{11} \\ a_{12} \end{pmatrix} \quad (1)$$

where  $a_i$ ,  $c_i$  and  $d_i$ ,  $b_i$  are amplitudes of the incident and reflected waves in the elements,  $S_1$  and  $S_2$  are the dispersion matrix of the energy feed device and H-plane tee with transmission coefficient  $h$  on the side of the side arm and

$$S_1 = \begin{pmatrix} -\sqrt{1-k^2} & jk \\ jk & -\sqrt{1-k^2} \end{pmatrix}, S = \begin{pmatrix} \frac{-1+\sqrt{1-h^2}}{2} & \frac{1+\sqrt{1-h^2}}{2} & \frac{h}{\sqrt{2}} \\ \frac{1+\sqrt{1-h^2}}{2} & \frac{-1+\sqrt{1-h^2}}{2} & \frac{h}{\sqrt{2}} \\ \frac{h}{\sqrt{2}} & \frac{h}{\sqrt{2}} & -\sqrt{1-h^2} \end{pmatrix} = \begin{vmatrix} s_{11} & s_{12} & s_{13} \\ s_{21} & s_{22} & s_{23} \\ s_{31} & s_{32} & s_{33} \end{vmatrix} \quad (2)$$

In addition, wave amplitudes in the system are connected with the following evident correlations:

$$\begin{aligned} a_1 &= d_2 e^{-0.5\alpha-0.5j\varphi}, c_2 = b_1 e^{-0.5\alpha-0.5j\varphi}, a_2 = -b_2 e^{-\beta-j\psi}, a_3 = b_6 e^{-0.5\gamma-j0.5\xi}, a_6 = b_3 e^{-0.5\gamma-j0.5\xi}, a_5 = -b_5 e^{-\beta-j\psi}, \\ a_4 &= b_7 e^{-0.5\alpha-0.5j\theta}, a_7 = b_4 e^{-0.5\alpha-0.5j\theta}, a_8 = -b_8 e^{-\beta-j\psi}, a_9 = b_{12} e^{-0.5\gamma-j0.5\kappa}, a_{10} = -b_{10} e^{-0.5\alpha-j0.5\chi}, a_{11} = -b_{11} e^{-\beta-j\psi}, \\ a_{12} &= b_9 e^{-0.5\gamma-j0.5\kappa} \end{aligned} \quad (3)$$

where  $\alpha, \beta, \gamma$ , and  $\varphi, \psi, \xi, \chi$  are, respectively, attenuation constants and phases of waves at the wave two-way traveling along the waveguide section between limiting tees and shorted straight and shared side arms of tees. Using (1)-(3), we can obtain expressions for wave amplitudes in all components of the system as the functions of transmission coefficient  $h$  and phasing constant in components:

$$b_6 = \frac{US_2}{1-VS_2}, b_2 = A + Bb_6, b_1 = s_{11}e^{-0.5\alpha-0.5j\varphi} - s_{12}e^{-\beta-j\psi}b_2 + s_{13}e^{-0.5\gamma-0.5j\xi}b_6, b_{12} = Rb_9$$

$$b_3 = Ud_2 + Vb_6, b_5 = Cb_7 + Db_3, b_8 = Eb_4 + Fb_{12}, b_9 = Jb_4 + Kb_{12}, b_{10} = \frac{(M-LP)b_9}{1-NL}, b_{11} = \frac{(P-MN)b_9}{1-NL}$$

$$b_7 = \frac{XS_1Ud_2}{(1-VS_2)(1-WS_1)}, d_2 = \frac{jk}{1+(1-k^2)^{0.5}} e^{-0.5\alpha-j\varphi} b_1, b_4 = \frac{Ud_2}{(1-VS_2)(1-WS_1)}, b_{10} = \frac{(M-LP)b_4}{(1-KR)(1-NL)}$$

c

$$A = \frac{s_{21}e^{-0.5\alpha-0.5j\varphi}}{1+s_{22}e^{-\beta-j\psi}}, B = \frac{s_{23}e^{-\beta-j\psi}}{1+s_{22}e^{-\beta-j\psi}}, C = \frac{s_{21}e^{-0.5\alpha-0.5j\theta}}{1+s_{22}e^{-\beta-j\psi}}, D = \frac{s_{23}e^{-0.5\alpha-0.5j\psi}}{1+s_{22}e^{-\beta-j\psi}}, F = \frac{s_{23}e^{-0.5\gamma-j0.5\kappa}}{1+s_{22}e^{-\beta-j\psi}}, E = C$$

$$G = s_{11}e^{-0.5\alpha-0.5j\theta} - s_{12}e^{-\beta-j\psi}E, H = s_{13}e^{-0.5\gamma-0.5j\xi} - s_{12}e^{-\beta-j\psi}F$$

$$U = s_{31}e^{-0.5\alpha-0.5j\varphi} - \frac{s_{32}s_{21}e^{-\beta-j\psi}e^{-0.5\alpha-0.5j\varphi}}{1+s_{22}e^{-\beta-j\psi}}, V = s_{33}e^{-0.5\gamma-0.5j\xi} - \frac{s_{32}s_{23}e^{-\beta-j\psi}e^{-0.5\gamma-0.5j\xi}}{1+s_{22}e^{-\beta-j\psi}}$$

$$\begin{aligned}
W &= s_{11}e^{-0.5\alpha-0.5j\theta} - \frac{s_{12}s_{21}e^{-\beta-j\psi}e^{-0.5\alpha-0.5j\theta}}{1+s_{22}e^{-\beta-j\psi}}, X = s_{13}e^{-0.5\gamma-0.5j\xi} - \frac{s_{12}s_{21}e^{-\beta-j\psi}e^{-0.5\gamma-0.5j\xi}}{1+s_{22}e^{-\beta-j\psi}} \\
J &= s_{31}e^{-0.5\alpha-0.5j\theta} - s_{32}e^{-\beta-j\psi}E, K = s_{33}e^{-0.5\gamma-0.5j\xi} - s_{32}e^{-\beta-j\psi}F \\
L &= \frac{s_{12}e^{-\beta-j\psi}}{1+s_{11}e^{-0.5\alpha-j0.5j\chi}}, M = \frac{s_{13}e^{-0.5\gamma-j\kappa}}{1+s_{11}e^{-0.5\alpha-j0.5j\chi}}, N = \frac{s_{21}e^{-0.5\alpha-j0.5j\chi}}{1+s_{22}e^{-\beta-j\psi}}, P = \frac{s_{123}e^{-0.5\gamma-j\kappa}}{1+s_{22}e^{-\beta-j\psi}} \\
R &= -s_{31}e^{-0.5\alpha-0.5j\chi} \frac{M-PL}{1-LN} - s_{32}e^{-\beta-j\psi} \frac{P-MN}{1-LN} + s_{33}e^{-0.5\gamma-0.5j\kappa} \\
S_1 &= s_{11}e^{-0.5\alpha-0.5j\theta} - \frac{s_{32}s_{21}e^{-\beta-j\psi}}{1+s_{22}e^{-\beta-j\psi}} + \left[ s_{13}e^{-0.5\alpha-0.5j\theta} - s_{12}s_{23}e^{-\beta-j\psi} \frac{e^{-0.5-0.5j\theta}}{1+s_{22}e^{-\beta-j\psi}} \right] \frac{JR}{1-KR} \\
S_2 &= s_{31}e^{-0.5\alpha-0.5j\theta} - \frac{s_{32}s_{21}e^{-0.5\alpha-0.5j\theta}e^{-\beta-j\psi}}{(1+s_{22}e^{-\beta-j\psi})} \frac{XS_1}{1-WS_1} + \left[ s_{33}e^{-0.5\gamma-0.5j\xi} - s_{23}s_{32}e^{-\beta-j\psi} \frac{e^{-0.5\gamma-0.5j\xi}}{1+s_{22}e^{-\beta-j\psi}} \right]
\end{aligned}$$

The obtained expressions will help us to find the behaviors of the system parameters dependencies in question. Thus, Figure 2 shows the dependencies of the wave power gain in the sections from the electrical length of the first section at different values of transmission coefficient  $h$  of the tee on the side of the side arm and two different lengths (quarter-wave or half-wave) of shorted straight arms. As is seen from the dependencies, the gain in sections is equal for all  $h$  (lines 1-3 и 4-6) at quarter-wave arms. However, this gain is reduced as  $h$  values become lower. For example, when  $h$  falls from 1 (the tee is matched on the side of the side arm) to 0.8 (the tee is not matched on the side of the side arm), the gain in sections drops by 50%, i.e. falls by 2 dB. The reason for this reduction becomes clear if we determine the gain distribution in all components of the system. The character of the distribution suggests that the gain reduction in the sections is connected with growing losses in the side arms due to the growth of the accumulated energy density. As  $h$  becomes lower, the low-Q cavity represented by the shared side arm increases the load on the main storing capacity of the system, i.e. the capacity of sections. When  $h$  falls from 1 to 0.8, the wave power in side arms grows from the half-power in the sections to the level two times higher. When  $h = 0.945$ , the wave powers are equal in the sections and side arms. In the given case all sections of the system and side arms of tees are half-wave ones. The coupling aperture transmission factor exceeded the optimal value for one section but was less than this value for three sections.

Changing the connection with the side arm results in changing the working frequency of the system. The same result is observed with different lengths of the sections. However, this difference does not influence the distribution of energy among sections. At the same time, when  $h$  is changed, the energy in the system is redistributed, which is manifested in the changes of energy correlations in side arms and sections.

After we change the length of a shorted quarter-wave arm to half-wave, the energy in the first section grows, while the stored energy in the section and third sections falls close to the zero level. This situation is shown by lines 7,8 and 9, respectively (Figure 2). This redistribution of energy can be obviously used for the formation of pulses of various shape, duration and gain, which is supported by the specific dependency of the gain in the parts of the resonant system element on the length of the shorted straight arm. As is seen from the dependencies in Figure 3, the change in the arm length exerts

strong influence on gain only near the half-wave length of the arm. This factor allows us to implement control of pulse parameter changes.

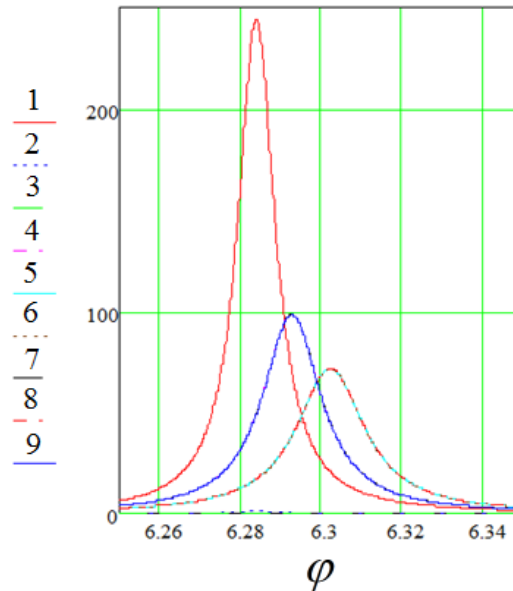


**Figure 2.** Dependencies of the wave power gain in the sections from the electrical length of the first section at different values of transmission coefficient of the tees on the side of the side tee and two different values of length  $\psi$  of shorted straight arms. Lines 1-3 and 4-6 –  $h=1, 0.8$  respectively,  $\psi = \pi/2$ ; line 7 –  $h=1, \psi = \pi$ , gain in the first section; lines 8,9 –  $h=1, \psi = \pi$ , gain in the second and third sections.

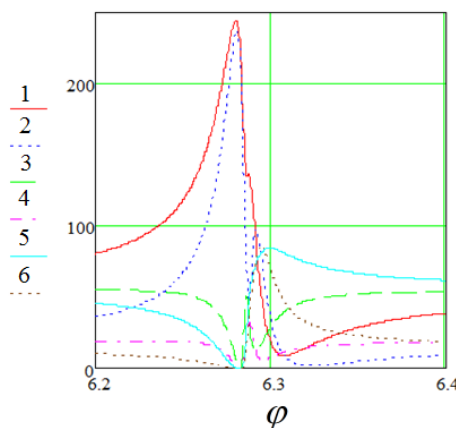


**Figure 3.** Dependencies of wave power gain in sections from the electrical length of a short-circuited arm near its half-wave length for a tee matched (lines 1-3) and unmatched on the side of the side arm.

After we change the length of a shorted quarter-wave arm to half-wave, the energy in the first section grows, while the stored energy in the section and third sections falls close to the zero level. This situation is shown by lines 7,8 and 9, respectively (Figure 2). This redistribution of energy can be obviously used for the formation of pulses of various shape, duration and gain, which is supported by

the specific dependency of the gain in the parts of the resonant system element on the length of the shorted straight arm. As is seen from the dependencies in Figure 3, the change in the arm length exerts strong influence on gain only near the half-wave length of the arm. This factor allows us to implement control of pulse parameter changes.

### 3. Experiments

As in work [1], the experimental studies were carried out using the S-band compression system with the planar-volumetric storage cavity designed as a meander but made of two structure elements (instead of three). Structure elements, as in work [1], were also designed as identical sections of a round waveguide with 90 mm diameter limited with H-tees made of the same waveguide (Figure 4). The coupling aperture was located on the input end of the first section. The second end was connected to the straight arm of the first limiting tee. The second straight arm of the tee was made with a quarter-wave length and was short-circuited. The side half-wave arm was connected to the corresponding arm of the limiting tee of the second section. The tee in the second section was connected with the tee in the third section in the same manner. Thus, the side arms of the section were connected in an integrated flat resonant system where each tee could be transformed into the energy extraction device. This could be simply performed by replacing the short-circuiter of the straight arm with an interference RF switch.

The main goal of the experiment was to demonstrate that this compression system could generate nanosecond rectangular pulses which would be longer than those described in work [1] and thus to prove the efficiency of the concept. For this purpose, the energy was extracted from the interference RF switch connected to the output end of the last (third) section. The switch tee was coplanar to the limiting tees, while the compression system output port was the open straight arm of the switch, and the closed half-wave side arm housed the MW switch. The switch tee on the side arm side was not matching and had the 0.8 transmission coefficient on the side of this arm. As in work [1], the switch in the switch unit was a trigatron RF discharge switch a vented gas discharge tube. The tube was in the electric field peak and oriented by the waveguide diameter in the plane of polarization of the transmitting wave. The electrical discharge switch of the lighting of the switch discharge gap was in one end of the tube.



**Figure 4.** Active microwave compression system with a compact storage cavity in the form of a meander.

At working frequency  $\sim 2800$  MHz, the cavity length was 650 mm from the axis of the one limiting tee side arm to the axis of another tee. The length of the shorted straight arm was  $\sim 110$  mm from the short circulator to the axis of the side arm, i.e. was close to the quarter-wave geometrical length of the arm. The total length of side arms between the axes of the section was  $\sim 178$  mm. With this length of

the sections and the shared arm of limiting tees, H11(31) oscillations were excited in the resonant cavity. Twenty seven half waves were in the sections and four half waves were in the shared arms.

The measured intrinsic Q-factor of the resonant cavity was  $\sim 2.1 \times 10^4$ . The estimated two-way travel time of the transmitted wave along all system components was  $\sim 20$  ns, while the maximum estimated gain coefficient of the compression system equal to the gain of the resonant cavity excited with the infinitely long pulse was equal to  $\sim 18$  dB. With account for the accumulation time limited with  $3 \mu\text{s}$  and the corresponding duration of the input pulse in the experiments with high power level and considering  $\sim 2$ -3 dB loss at the extraction, the anticipated gain coefficient was  $\sim 14$ -15 dB.

The magnetron oscillator with pulse power up to  $\sim 2$  MW was used as a source of input pulses. The insulating gas in the cavity was gaseous nitrogen at 3-4 ATMG with 10-12% insulating gas. Switching to output mode was performed in the argon medium in the discharger tube under pressure 2-3 ATMG or in the mixture of argon with  $\sim 5$ -10% insulating gas at 0-1 ATMG.

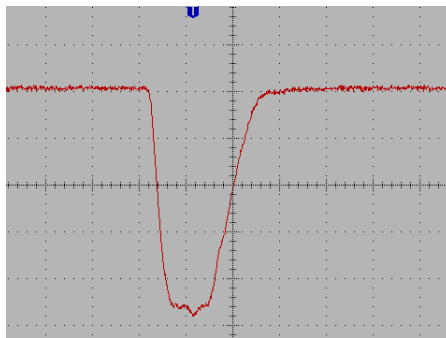


**Figure 5.** Oscillogram of the output pulse of the RF compression system with switching in argon with 7-10% insulating gas: gain 13 dB, power 40 MW, duration 25 ns.

Figure 5 shows the oscillogram of a RF pulse with a nearly rectangular form generated by the compression system. The pulse reached 13 dB gain, 24-25 ns duration and approximately 40 MW power. The pulses were formed with switching in argon with a relatively significant share of insulating gas. When the share of insulating gas was decreased up to its complete removal from the mixture, the pulse shape was deformed, as shown in the oscillograms in Figure 6. An adequately supported explanation of such deformation has not been found yet. The reason for the distortion of the pulse shape will be the subject of further research.

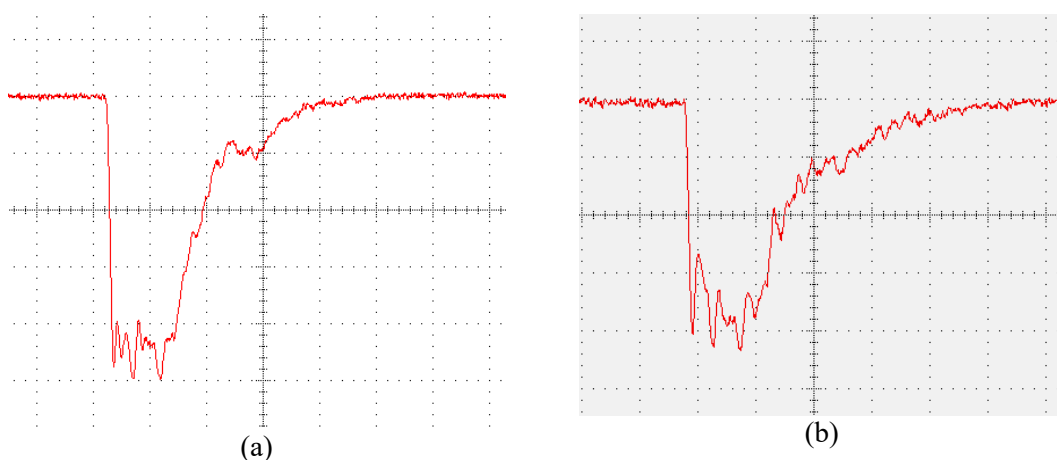


**Figure 6.** Oscillograms of output pulses at different switching conditions, (a) in argon; (b) in argon with 5-7% insulating gas.

#### 4. Summary and Conclusions

The paper summarizes the study of the active microwave pulse compression system with energy storage in the resonant system made in the form of a meander. Due to such form, the system has relatively small dimensions and the wave travel time in the system is much larger than the travel time in the system of maximum dimensions. The system is designed on the basis of the structure element made as a waveguide section whose ends are limited with two H-tees. The connection of the sections through tees allows building the resonant cavity as a one-, two- or three-dimensional structures. It was proved that the compression system of this kind is capable of generating pulses with the pulse shape very close to rectangular and the length of the radiated wave train several times exceeding the compression system dimensions. In fact, these configurations are a set of traditional RF compression systems based on H-tees aligned along a straight line, either in one plane or in three dimensions. Due to this approach, we can build compact active RF compression systems that can generate long rectangular nanosecond pulses and can be fitted effectively into the RF unit.

#### Acknowledgments

This work was supported in part in the scope of the Program on National Research Tomsk Polytechnic University Competitiveness Enhancement Program and partially supported by grant RFBR № 15-08-01853.

#### References

- [1] Artemenko S, Beverly III R, Gorev S, Igumnov V, *Proceedings of 2016 IEEE International Power Modulator and High Voltage Conference*, 2016
- [2] Altman J L, *Microwave Circuits*, Princeton 1964, N.J.: Van Nostrand